(solvus lines only shown as dashed lines in Figure 3).

These three binary diagrams depict sides of a right triangular prism chosen to describe the temperature–composition relationships in the ternary system. A polythermal projection on the composition plane was adopted to describe the liquidus surfaces of the ternary system (Figure 4).

The eutectic valleys were found by measuring the solid–liquid equilibria along internal sections of the ternary diagram (*4*). Some characteristic points are listed in Table III.

The ternary system shows an invariant eutectic point at 102 K, with composition (in mole fraction) 0.287 1,8-cineole, 0.325 (−)-α-pinene, such composition having been estimated by perspective projections of the eutectic valleys (*5*).

In summary, Figure 4 shows that from the viewpoint of 1,8-cineole production more than 80% of the area of the ternary diagram can be used, thus exceeding by far the range of temperatures available for industrial purposes. In this study, low-temperature determinations were made difficult by glass-type transitions (whenever the increase in viscosity prevented stirring), which were responsible for the decrease in accuracy as temperature was lowered.

Registry No. 1,8-Cineole, 470-82-6; (+)-limonene, 5989-27-5; (−)-α-pinene, 7785-26-4.

Literature Cited

(1) Goates, J. R.; Ott, J. B.; Budge, A. H. *J. Phys. Chem.* **1961**, *65*, 2162.
(2) van Wijk, H. F.; Smit, W. M. *Anal. Chim. Acta* **1960**, *23*, 545.
(3) van Wijk, H. F.; Smit, W. M. *Anal. Chim. Acta* **1961**, *24*, 41.
(4) Tamás, F.; Pál, I. *Phase Equilibria Spatial Diagrams*, 1st ed.; Butterworth: Budapest, 1970; Chapter III.
(5) Ricci, J. E. *The Phase Rule* and *Heterogeneous Equilibrium*; Dover: New York, 1966; p 315.

Received for review December 29, 1986. Accepted October 26, 1987. This work was sponsored by the Instituto Nacional de Investigação Científica and by Fundação Calouste Gulbenkian, Portugal. We thank Cirel, L. Pastora, Portugal, for kindly supplying the (+)-limonene used in this work.

Effect of Pressure on the Constant-Pressure Heat Capacity of a Methane–Carbon Dioxide Mixture

James R. Boulton and Fred P. Stein*
Chemical Engineering Department, Lehigh University, Bethlehem, Pennsylvania 18015

The constant-pressure heat-capacity ratio, $C_{p_{HP}}/C_{p_{1atm}}$ (where $C_{p_{HP}}$ is the heat capacity at high pressure and $C_{p_{1atm}}$ the heat capacity at 1 atm), was measured for a 49.2 mol % mixture of methane in carbon dioxide along isotherms of 302.2, 312.7, and 325.2 K at pressures between 7 and 60 bar. No maximum in the heat capacity was encountered. The largest heat-capacity ratio (1.399, 1.340, and 1.263 for each isotherm, respectively) occurred at 60 bar. The uncertainty in the heat-capacity ratios is estimated to be 0.6%. The data were compared to heat-capacity ratios calculated from the Soave–Redlich–Kwong equation of state.

Introduction

Wherever nonidealities are significant in an energy balance applied to the design and analysis of process equipment, ideal-gas heat capacities are used in conjunction with enthalpy departures calculated from an equation of state (EOS). Even if constant-pressure heat capacities (C_p) for gases at high pressure were available, it is unlikely that they would be used directly in such process analysis. However, high-pressure C_p's would be very valuable for adjusting the parameters in the EOS subsequently used in the process analysis.

The direct calorimetric measurement of C_p at high pressure is a very difficult task, which explains the paucity of such data, but the measurement of the ratio of C_p at high pressure to C_p at 1 atm is, *relatively* speaking, easy. We have adopted the heat-exchange method for measuring the C_p ratio. This method was first used by Workman (*1*, *2*) in 1930 for oxygen, nitrogen, and hydrogen. Interest in the Workman calorimeter was revived in 1970 by Balaban and Wenzel (*3*) who studied nitrogen–trifluoromethane mixtures. Shortly thereafter, Bishnoi and Robinson (*4*, *5*) reviewed the available equipment and used the Workman calorimeter to study carbon dioxide–methane mixtures. Bishnoi et al. (*6*) and Hamaliuk et al. (*7*) studied nitrogen–carbon dioxide mixtures and nitrogen–hydrogen sulfide mixtures, respectively.

In the Workman calorimeter, the C_p ratio can be measured without measuring the flow rate (or mass) of the gas and without worrying about the heat leak, or its size, as long as it is reasonably small. The C_p at high pressure, then, is readily available because the C_p at 1 atm is known for many materials, or, for a mixture, it can be calculated from the ideal-gas C_p's of the constituents.

The difference between a high-pressure C_p and the ideal-gas C_p at the same temperature is related to the pressure–volume–temperature (*PVT*) properties of the gas, that is, related to an EOS. Thus, the data presented here afford an opportunity to test different aspects of an EOS than the usual tests provided by *P*–*V*–*T* and vapor–liquid equilibrium measurements. We elected to compare calculations of the C_p ratio from the Soave–Redlich–Kwong EOS to the data.

Experimental Section

Materials. The gas mixture used in these experiments was 49.2 ± 0.4 mol % methane in carbon dioxide, as determined by gas chromatographic (GC) analysis using composition standards traceable to the U.S. National Bureau of Standards. GC analysis which focused on the impurities showed 14 ppm (molar) ethane and about 0.7 ppm ethylene. Periodically during the measurements, samples were removed from the apparatus and checked by GC for any air that may have contaminated the test gas during loading or operation. No air was detected in any of the samples; the limit of detectability was 0.05%.

Apparatus. The method used for experimentally determining the Cp ratios in the form $C_{p_{HP}}/C_{p_{1atm}}$ was first used by Workman (*1*). A schematic of the apparatus is shown in Figure 1; the details are available elsewhere (*8*).

The measurements were made in the countercurrent-flow heat exchanger in which the test gas passes through one side at high pressure and through the other side at 1 atm. Because

0021-9568/88/1733-0196$01.50/0

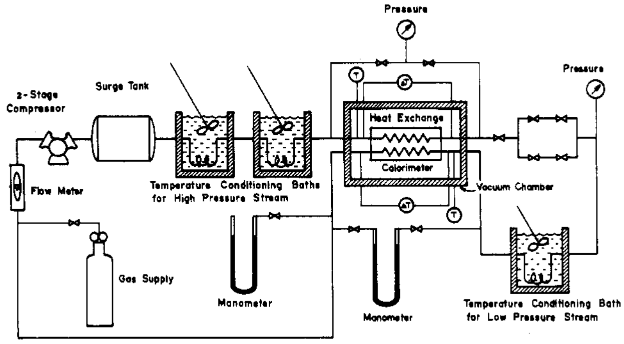

Figure 1. Schematic of the heat-exchange calorimeter.

the test gas is contained in a closed circulation loop, the mass flow rate on each side of the exchanger is the same, and it effectively cancels out of the energy balance. The temperatures of the two gas streams entering the heat exchanger were adjusted to the desired levels for a given measurement, and then fine tuned relative to each other such that the high-pressure stream underwent a temperature change of 4.00 ± 0.02 K. The key measurements are the changes in temperature of the high-pressure stream (ΔT) and the low-pressure stream (ΔT^*) through the exchanger. The energy balance for the case where the high-pressure stream is being heated is

$$C_{p_{\mathrm{HP}}}\Delta T + C_p{}^*\Delta T^* = \theta_{\mathrm{H}} \tag{1}$$

where the term θ_{H} is primarily, but not solely, the heat leak divided by the mass flow rate; θ_{H} also includes provisions for the small effects of pressure drop on the energy of the flowing streams.

As first outlined by Workman (*1*) and shown in greater detail by Boulton (*8*), if (a) the temperatures of the gas streams entering the heat exchanger are adjusted so that the high-pressure stream is (now) cooled over exactly the same ΔT at the same mean temperature as it was previously heated and if (b) the heat leak per mass flow is the same in both the high-pressure heating and cooling experiments, then exactly the same energy balance shown in eq 1 is obtained with the important exception that each term in θ_{H} has exactly the opposite sign. Thus, adding the two energy balances, one for heating the high-pressure stream and the other for cooling it, produces the working equation for the measurement of the C_p ratio

$$\frac{C_{p_{\mathrm{HP}}}}{C_{p_{\mathrm{1atm}}}} = \frac{1}{2}\left[\frac{-\Delta T^*}{\Delta T}\ \text{(heating the HP stream)} + \frac{-\Delta T^*}{\Delta T}\ \text{(cooling the HP stream)}\right] \tag{2}$$

The only measurements required are the temperature differences. And, of considerable significance, no flow-rate (mass) measurements nor heat-leak estimates are required.

The test gas is compressed and circulated through the apparatus by a two-stage Corblin diaphragm compressor. The diaphragms permit compression of the test gas without any contact or contamination by lubricants. The gas flows from the compressor through two constant-temperature baths in series before entering the high-pressure side of the exchanger at the desired temperature. Immediately after leaving the high-pressure side of the heat exchanger, the pressure of the gas is reduced to 1 atm through a series of valves. The temperature of the gas entering the low-pressure side of the heat exchanger is then adjusted to its desired value in another constant-temperature conditioning bath. After passing through the low-pressure side, the test gas returns to the compressor.

The temperature differences of the high- and low-pressure streams across the exchanger were measured with thermopiles that had been calibrated to ±0.02 K with a platinum resistance thermometer that has a certification traceable to the U.S. National Bureau of Standards. The inlet temperatures of the high- and low-pressure streams were measured with thermocouples that had been calibrated to ±0.02 K with the same standard. The emfs were read to the necessary precision and accuracy on a Leeds and Northrup Type K-5 potentiometer. The pressure on the high-pressure stream was read on a Heise bourdon gauge to ±0.5 psia. The gauge had been previously calibrated with a Ruska deadweight gauge using class "s" weights that were certified by Ruska as traceable to the U.S. National Bureau of Standards. The pressure on the low-pressure stream was read on a mercury manometer to within ±0.5 mmHg.

Table I. C_p Ratio for the CH_4–CO_2 Mixture at 302.2 K

press., bar	$C_{p_{\mathrm{HP}}}/C_{p_{\mathrm{1atm}}}$ exptl	SRK	press., bar	$C_{p_{\mathrm{HP}}}/C_{p_{\mathrm{1atm}}}$ exptl	SRK
6.89	1.009	1.028	37.92	1.199	1.199
10.34	1.030	1.043	41.37	1.225	1.224
13.79	1.050	1.059	44.81	1.252	1.251
17.24	1.070	1.076	48.26	1.281	1.279
20.68	1.091	1.094	51.71	1.312	1.308
24.13	1.111	1.112	55.16	1.346	1.340
27.58	1.132	1.132	58.60	1.383	1.373
31.02	1.153	1.153	59.98	1.399	1.387
34.47	1.176	1.176			

Table II. C_p Ratio for the CH_4–CO_2 Mixture at 312.7 K

press., bar	$C_{p_{\mathrm{HP}}}/C_{p_{\mathrm{1atm}}}$ exptl	SRK	press., bar	$C_{p_{\mathrm{HP}}}/C_{p_{\mathrm{1atm}}}$ exptl	SRK
6.89	1.032	1.025	37.92	1.179	1.174
10.34	1.044	1.039	41.37	1.201	1.194
13.79	1.057	1.053	44.81	1.225	1.216
17.24	1.071	1.068	48.26	1.249	1.239
20.68	1.086	1.084	51.71	1.274	1.262
24.13	1.103	1.100	55.16	1.301	1.287
27.58	1.120	1.117	58.60	1.329	1.313
31.02	1.139	1.135	59.98	1.340	1.324
34.47	1.159	1.154			

To minimize heat leak to or from the surroundings, the entire heat exchanger was housed inside a vacuum vessel filled with perlite powder and evacuated to 0.03 mmHg. In addition, water at the mean temperature of the high-pressure stream was circulated through copper tubing wrapped spirally around the vacuum vessel and intimately attached to it. Finally, the outside of the vacuum vessel was insulated with fiberglass and rock wool.

For each isotherm, 10–12 measurements of $\Delta T^*/\Delta T$ were taken between 7 and 62 bar when the high-pressure stream was being heated and another 10–12 points of $\Delta T^*/\Delta T$ were taken when the high-pressure stream was being cooled. These data for heating and for cooling were then fit to third-degree polynomials, and the C_p ratios were determined from the mean values between the two curves, as required by eq 2.

The apparatus was proof tested with nitrogen at 312.7 K over the pressure range from 13 to 83 bar where the C_p ratios ranged from 1.021 to 1.116. Agreement with Balaban's data (*9*) along the same isotherm was within less than 0.6%. The data obtained also agree to within less than 0.8% of the C_p ratios calculated from the Soave–Redlich–Kwong EOS.

Results

Three isotherms at 302.2, 312.7, and 325.2 K were investigated for a 49.2 mol % mixture of methane in carbon dioxide over a pressure range from 7 to 62 bar. The experimentally determined heat-capacity ratios are presented in Tables I–III. For all three isotherms, the C_p ratio was close to unity at 7 bar and increased steadily with pressure. The largest ratios measured were 1.399, 1.340, and 1.275 for the 302.2, 312.7, and 325.2 K isotherms, respectively. For any particular pressure,

Table III. C_p Ratio for the CH_4-CO_2 Mixture at 325.2 K

press., bar	$C_{p\mathrm{HP}}/C_{p\mathrm{1atm}}$ exptl	$C_{p\mathrm{HP}}/C_{p\mathrm{1atm}}$ SRK	press., bar	$C_{p\mathrm{HP}}/C_{p\mathrm{1atm}}$ exptl	$C_{p\mathrm{HP}}/C_{p\mathrm{1atm}}$ SRK
6.89	1.021	1.023	37.92	1.147	1.149
10.34	1.033	1.035	41.37	1.164	1.166
13.79	1.046	1.047	44.81	1.180	1.184
17.24	1.060	1.060	48.26	1.198	1.202
20.68	1.073	1.074	51.71	1.216	1.221
24.13	1.087	1.088	55.16	1.235	1.241
27.58	1.102	1.102	58.60	1.255	1.261
31.02	1.116	1.117	59.98	1.263	1.269
34.47	1.132	1.133	62.05	1.275	1.282

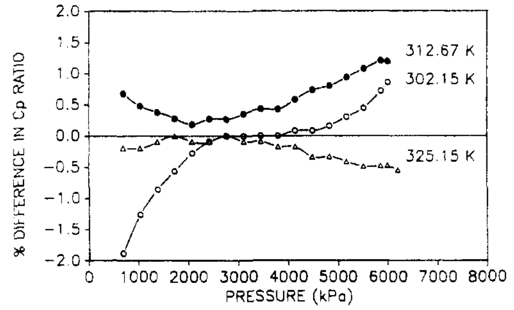

Figure 2. Percentage difference between experimental and SRK-predicted C_p ratios.

the C_p ratio was greater for a lower temperature isotherm.

The uncertainty in the data is approximately 0.6% over most of the pressure range. Only at heat-capacity ratios less than about 1.05 does the uncertainty in temperature-difference measurements lead to larger overall uncertainties.

Discussion

For purposes of comparison, the C_p ratios of the test mixture were calculated by applying the Soave-Redlich-Kwong (SRK) EOS (*10*) to the rigorous thermodynamic equation

$$C_p = C_p^* - \left(R + T\frac{\left(\frac{\partial P}{\partial T}\right)_V}{\left(\frac{\partial P}{\partial V}\right)_T}\right) - T\int_V^{\infty}\left(\frac{\partial^2 P}{\partial T^2}\right)_V \mathrm{d}V \qquad (3)$$

The mixing rules suggested by Soave (*10*) were used along with one temperature-independent binary interaction parameter in the attractive term. The value ($k_{ij} = 0.0933$) was obtained from a compilation by Knapp et al. (*11*) based on vapor-liquid equilibria (VLE).

The expressions given by Reid et al (*12*) for the ideal-gas heat capacity, C_p^*, of methane and carbon dioxide were combined according to the mole fractions of each to give C_p^* for the mixture. This value was set equal to $C_{p\,\mathrm{1atm}}$, as required in eq 2, without correction.

The results of the SRK calculations are shown in Tables I-III and in Figure 2. The difference plot shows that agreement with the experimental results is quite good. At the lowest pressures, where the precision of the experimental data is poorest because the C_p ratio is near unity, the differences result from scatter in the experimental data. At high pressures the agreement is excellent and within experimental error for much of the pressure range even though a k_{ij} based on VLE data was used for the heat-capacity predictions. Regression of these experimental heat-capacity data for a special k_{ij} would result in a fit that is well within experimental error even at 62 bar. However, the preferred procedure for fitting any equations of state and mixing rules would be the regression of $P-V-T$ and VLE data along with the heat-capacity data (*13*).

Registry No. CH_4, 74-82-8; CO_2, 124-38-9.

Literature Cited

(1) Workman, E. J. *Phys. Rev.* **1930**, *36*, 1083.
(2) Workman, E. J. *Phys. Rev.* **1931**, *37*, 1345.
(3) Balaban, S. M.; Wenzel, L. A. *Ind. Eng. Chem. Fundam.* **1970**, *9*, 568.
(4) Bishnoi, P. R.; Robinson, D. B. *J. Basic Eng.*; *Trans. A.S.M.E.* **1972**, 757.
(5) Bishnoi, P. R.; Robinson, D. B. *Can. J. Chem. Eng.* **1971**, *49*, 657.
(6) Bishnoi, P. R.; Hamaliuk, G. P.; Robinson, D. B. *Can. J. Chem. Eng.* **1972**, *50*, 677.
(7) Hamaliuk, G. P.; Bishnoi, P. R.; Robinson, D. B. *J. Chem Eng. Data* **1974**, *19*, 78.
(8) Boulton, J. R. M.S. Thesis, Lehigh University; Bethlehem, PA, 1966.
(9) Balaban, S. M. Ph.D. Thesis, Lehigh University, Bethlehem, PA, 1966.
(10) Soave, G. *Chem. Eng. Sci.* **1972**, *27*, 1197.
(11) Knapp, H.; Doring, R.; Oellrich, L.; Plocker, U.; Prausnitz, J. M. *Vapor-Liquid Equilibria for Mixtures of Low Boiling Substances*; DECHEMA: Frankfurt/Main, 1982; p 773.
(12) Reid, R. C.; Sherwood, T. K.; Prausnitz, J. M. *The Properties of Gases and Liquids*; McGraw-Hill: New York, 1977; Appendix A.
(13) Naheiri, T.; Mathias, P. M.; Copeman, T. W. "Impact of Calorimetry on Process Design", presented at 42nd Annual Calorimetry Conference, Boulder, CO, July 26-31, 1987.

Received for review November 26, 1986. Accepted December 30, 1987.

Mixture Densities of Aqueous KCl with NaCl up to Ionic Strength 4.5 mol kg^{-1} and at 298.15 K

Anil Kumar

Department of Sugar Chemistry, Deccan Sugar Institute, Manjari (Bk) 412 307, Poona, India

The experimental density differences, Δd, are reported for aqueous mixtures of KCl with NaCl at 298.15 K from the constant ionic strength, I, 0.5-4.5 mol kg^{-1} of water. The results are fitted to the equations derived by Patwardhan and Kumar (equivalent to Young's rule) and by Pitzer. The interactions between Na^+ and K^+, as shown by the excess volumes, ΔV_m, are very small.

Introduction

In continuation of our work on the volume properties of concentrated electrolyte mixtures (*1*, *2*), we now present the experimental density differences for aqueous KCl-NaCl at 298.15 K. Wirth (*3*) and Millero and Sotolongo (*4*) have also reported the densities of this system, but their measurements were restricted to the ionic strength, I, of 1.5 mol kg^{-1} of water. This article reports the experimental density differences, Δd, for this system at constant I = 0.5, 1, 2, 3, and 4.5 mol kg^{-1}, ranging from pure KCl to pure NaCl solutions.

Experimental Section

Both KCl and NaCl from BDH (AR Grade), dried in an oven, were directly used for preparing the stock and starting solutions.

0021-9568/88/1733-0198$01.50/0